Journal of Elementology ISSN 1644-2296

Li Y., Chen Y., Karimian H., Tao T. 2020.
Spatiotemporal analysis of air quality and its relationship with meteorological factors in the Yangtze River Delta.
J. Elem., 25(3): 1059-1075. DOI: 10.5601/jelem.2019.24.4.1931

RECEIVED: 9 November 2019
ACCEPTED: 27 May 2020

ORIGINAL PAPER

SPATIOTEMPORAL ANALYSIS OF AIR QUALITY AND ITS RELATIONSHIP WITH METEOROLOGICAL FACTORS IN THE YANGTZE RIVER DELTA

Yaqian Li[1↓], Youliang Chen[1], Hamed Karimian[1↓], Tianhui Tao[2]

**[1] School of Architectural and Surveying and Mapping Engineering
Jiangxi University of Science and Technology, Ganzhou, China
[2] College of Surveying and Geo-Informatics
Tongji University, Shanghai, China**

Abstract

Air quality is closely related to people's health and life. In addition to being directly affected by social activities and atmospheric emissions, the impacts of meteorological factors are also significant. Based on daily Air Quality Index (AQI) data and various meteorological parameters in the Yangtze River Delta (YRD), this paper summarized the spatiotemporal evolution characteristics of AQI over YRD, and quantitatively analyzed the contribution of different meteorological elements to air quality. We also evaluated different spatial interpolation methods to produce surface distribution of AQI, and noted that the Ordinary Kriging outperformed other methods. The spatial distribution of AQI in YRD showed seasonal and annual variations. However, the days with AQI over 100 (level ii) were mostly observed in winter. Generally, more severe air pollution was observed in the northern part of YRD than in the southern ones, for example the air quality of the Ningbo metropolitan area was the best, while in Hefei it was the worst. It was found that meteorological parameters have spatially varying effects on AQI. For instance, pressure has a significant positive effect on AQI, and others showed negative correlations. We also predicted AQI by exploiting different machine learning-based models. Through model comparison, it was found that the Autoregressive Integrated Moving Average Model – ARIMA (0,1,2) has higher prediction accuracy for AQI than Multiple Linear Regression (MLR). The findings of this research can be used in future forecasting of air pollution, and also in air pollution controlling programs.

Keywords: YRD, air quality index, meteorological elements, correlation analysis, air pollution, spatial analysis.

Youliang Chen, School of Architectural and Surveying& Mapping Engineering, Jiangxi University of Science and Technology, Ganzhou 341000, China, e-mail: 9120010023@jxust.edu.cn; phone: +86- 13970782005
↓ These Authors contribute equally to this work.

INTRODUCTION

With the rapid development of economy, environmental problems have become more prominent. Among them, the atmospheric environment is closely related to human life, and urban air quality has become a growing concern (Chwil et al. 2015, Mo et al. 2020), especially in areas with high-density populations (Li et al. 2017). Air quality is the result of a change in atmospheric pollutants, which has adverse effects on the human body and ecological health (Nowak et al. 2018). Therefore, it is crucial to gain comprehensive and objective understanding of air quality, which can also provide a scientific basis for effective management and air pollution controlling programs. Meteorological conditions directly affect the dispersion, transportation, formation and deposition of atmospheric pollutants, which play an important role in air pollution. At present, many scholars conduct extensive research on air quality distribution and its relationship with meteorological factors. Baltaci et al. (2019) found that considering meteorological parameters such as temperature, relative humidity, precipitation, and atmospheric circulation can hepl to explain better changes in air pollution. Based on an analysis of data obtained from 5 monitoring stations, Hrishikesh and Nagendra (2019) explored the effects of the weather and wind speed on air pollutant concentrations in Chennai city. Spatiotemporal variation of the influence of wind on the distribution of fine particulate matter and its precursor gases was investigated by Karimian et al. (2019). Their results showed that the influence of wind on the concentration of particulate matter and its precursor gases varies spatially over Beijing, Borge et al. (2019) evaluated the impact of meteorological parameters (temperature, wind speed, humidity and precipitation) on air pollutants (C_6H_6, CO, NO_2, NO_x, O_3, PM_{10}, $PM_{2.5}$) in Spain, and the results showed that the weather has a significant impact on PM_{10}. Based on the mean sea level pressure and wind field data of ERAS (European Centre for Medium-Range Weather Forecasts), Adame et al. (2019) report the evolution of tropospheric NO_2 over the south-east of the Iberian Peninsula from 2005 to 2017. Adaes and Pires (2019) used Artificial Neural Networks (ANN) defined by Genetic Algorithms (GA) to evaluate the influence of meteorological variables and PM_{10} on $PM_{2.5}$ concentrations in Istanbul. Fenech et al. (2019) examined the meteorological drivers resulting in concurrent, high levels of ozone and PM2.5 during two five-day air pollution episodes in 2006 (1^{st} - $5t^{h}$ July and 18^{th} - 22^{nd} July) in the UK. The results show that both episodes were driven by anticyclonic conditions with light easterly and south easterly winds and high temperatures. Li et al. (2017) found that precursor gases followed by favorable meteorological conditions have a direct effect on concentrations of ozone in Hangzhou. Li et al. (2018) studied three-dimensional distributions of ozone and $PM_{2.5}$ concentrations in Shanghai, and found that temperature, relative humidity and atmospheric pressure are the major parameters that affect the variations of ozone and $PM_{2.5}$. Zhang et al.

(2018) discussed the spatial-temporal distribution characteristics of $PM_{2.5}$ in Anhui, and investigated the key influencing factors of $PM_{2.5}$ concentrations. They found that the population, urbanization rate, annual average temperature, unit Gross Domestic Product (GDP) power consumption and numbers of treatment facilities for industrial waste gas play a fundamental role in reducing $PM_{2.5}$ concentrations.

The rapid development of industrialization and transportation has strengthen the relationship between cities, and air quality reflects regional characteristics. Therefore, combining Air Quality Index (AQI) with urban agglomeration creates a trend in the expolration of the characteristics of air quality (Zheng et al. 2018). This research focuses on the new Yangtze River Delta (YRD) urban agglomeration, which covers three provinces and a city (Jiangsu, Zhejiang, Anhui, Shanghai). For such a large geographical area as YRD, which has significant population density (over 150 million) with rapid urbanization and economic growth, exploring air quality conditions and the influencing parameters are the essential for air pollution controlling programs. In this research, we implemented a statistical analysis to investigate the spatial and temporal variation characteristics of air pollution and its correlation with different meteorological parameters in the past five years. Moreover, we proposed a statistical model to predict AQI over YRD.

MATERIALS AND METHODS

Study area

The Yangtze River Delta is an alluvial plain, covering a land area of 211,700 square kilometers (almost 2.2% of China's total land territory), where there are 26 cities. The YRD urban agglomeration (one core and five circles) includes Nanjing Metropolitan Circle, Suzhou-Wuxi-Changzhou Metropolitan area, Hangzhou Metropolitan Circle, Ningbo Metropolitan Circle, Hefei Metropolitan Circle, and Shanghai Core Area. Due to the wealth of regional resources and high energy consumption, various atmospheric pollutants at different concentrations are observed over the area, causing severe environmental problems (Wang et al. 2018).

According to the Environmental Protection Website of the People's Republic of China, there are 89 monitoring stations in the cities covered by the "one core and five circles" in YRD. Figure 1 illustrates the study area (one core and five circles) and the location of 89 air pollution monitoring stations.

ARIMA model

The Autoregressive Moving Average – ARMA (p, q) model is currently the most commonly used stationary time series model (Eq. 1). This model

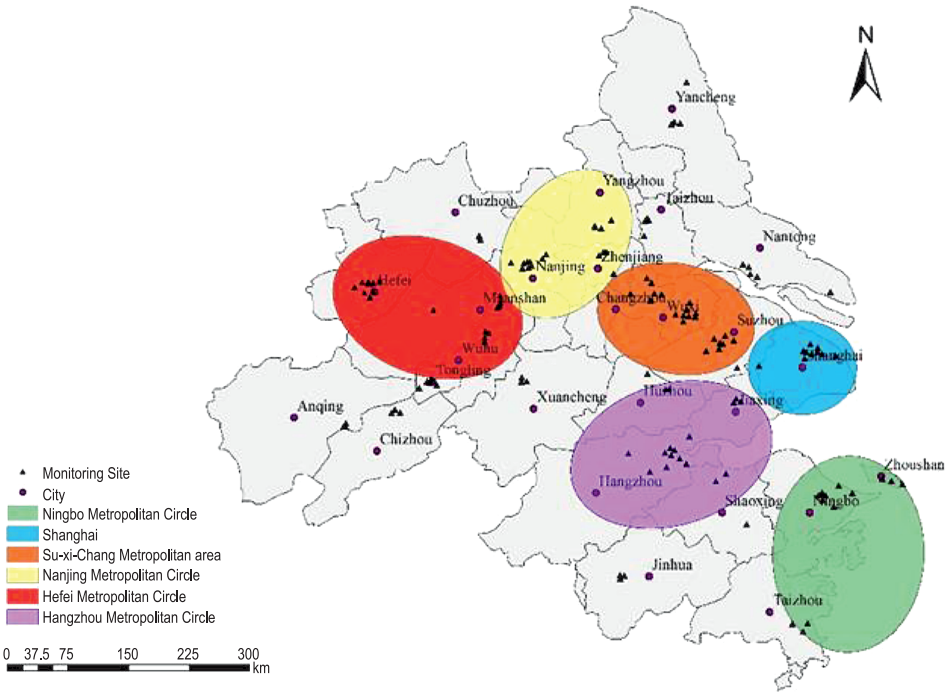

Fig. 1. Spatial distribution of air pollution monitoring stations in one core (Shanghai) and 5 circles

is a mix of the Autoregressive model of order p and the moving average model of order q.

$$Y_t = \Phi_1 Y_{t-1} + \Phi_2 Y_{t-2} + \cdots + \Phi_p Y_{t-p} + e_t - \Theta_1 e_{t-1} - \Theta_2 e_{t-2} - \cdots - \Theta_q e_{t-q} \quad (1)$$

In the above equation, denotes the value of the time series Y at time step t. e_t, e_{t-1}, … e_{t-q} stand for the model errors, Φ_1, Φ_2, … Φ_p are the autoregressive coefficients and Θ_1, Θ_2, … Θ_q, are moving average coefficients. If the d-order difference ($W_t = \nabla^d Y_t$) of a time series $\{Y_t\}$ is a stationary ARMA process, then $\{Y_t\}$ is called the Autoregressive Integrated Moving Average Model (ARIMA). In this study, we used the IBM SPSS Statistics 21 software to run the model.

As mentioned earlier, the ARIMA is a stationary time series model. However, the AQI time series is a non-stationary sequence. After the first--order difference was achieved, the AQI sequence was stabilized and the unit root test was performed. Therefore, the order of our proposed ARIMA model is d=1. In order to find the optimal parameters (p, q), the Auto-correlation function (ACF) map and the Partial auto-correlation function (PACF) map are combined with the Akaike minimum information criterion (AIC) and the Schwarz-Bayes criterion (BIC). From the characteristics of the ACF and PACF of the difference sequence, the autocorrelation coefficients of the five

cities are censored, and the partial autocorrelation coefficients exhibit tailing. After trial and error and model screening, AR (p=0) and MA (q=2) were selected for the difference sequence.

Spatial interpolation

The best way to convert point-scale data to polygon-scale information is spatial interpolation. Spatial interpolation includes the evaluation of interpolation accuracy and the selection of interpolation methods. To perform spatial interpolation of our data, we used ArcGIS software to compare the accuracy of Ordinary Kriging (OK), Inverse Distance Weighted (IDW) and Global Polynomial Interpolation (GPI) – Table 1. The Kriging method provides an unbiased optimal estimation of the value of variables in a finite region, considering not only the distance, but also the spatial distribution of the known sample points and the spatial azimuth relationship with the unknown sample points through the variation function and structure analysis. The Kriging interpolation equation can be expressed as:

$$Z(X_0) = \sum_{t-1}^{n} \lambda_i Z(X_i) \tag{2}$$

where: $Z(X_0)$ – value of an unknown point $Z(X_i)$ – value of the known points around the unknown point, λ_i – weight of *ithe*-known sample point with respect to its distance to unknown sample point, and n – number of known sample points.

The inverse distance weighted interpolation equation can be expressed as:

$$\nu = \sum_{j=1}^{N} = \frac{1}{(d_j)^p} \nu(x_j) / \sum_{j=1}^{N} \frac{1}{(d_j)^p} \tag{3}$$

where: ν – estimated value, N – number of sample points, d_j – the distance between the interpolation point and the *ithe*-known sample point, p – specified power.

The indicators for evaluating interpolation accuracy are Mean Standardized Error (MSE) and Root Mean Square Error (RMSE).

$$MSE = \frac{\sum_{j=1}^{N} abs(Z_i - Z_j)}{n} \tag{4}$$

$$RMSE = \sqrt{\frac{\sum_{i=1}^{N} (Z_i - Z_j)^2}{n}} \tag{5}$$

where: n – number of air monitoring stations, Z_i – known as the station point of AQI, Z_j – interpolated point of AQI.

RESULTS AND DISCUSSIONS

Spatial and temporal distribution characteristics of air quality

Comparison of air quality and air pollutants in different time periods

Figure 2 illustrates the AQI level distribution for different regions of the YRD urban agglomeration. In total, there are 1,815 days with valid

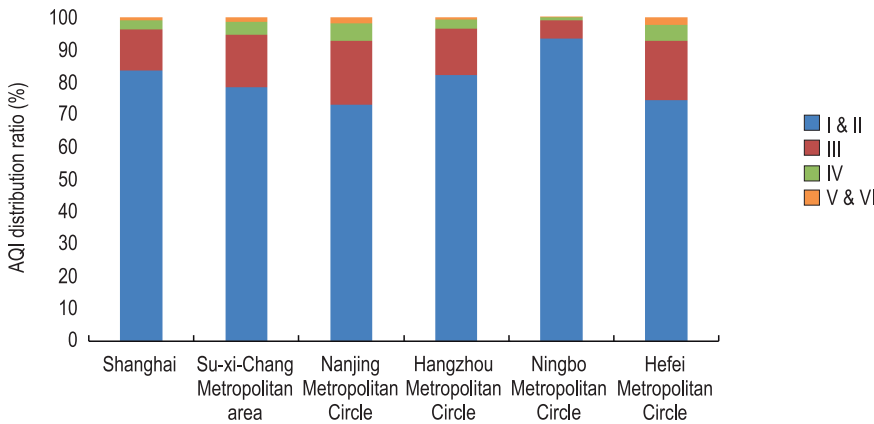

Fig. 2. AQI level distribution in different regions of YRD

data. During our study period (5 years), the number of air pollution days in Shanghai is 301 days, Suzhou-Wuxi-Changzhou Metropolitan area – 393 days, Nanjing Metropolitan Circle – 493 days, Hangzhou Metropolitan Circle – 324 days, Ningbo metropolitan circle – 120 days, and Hefei Metropolitan Circle – 466 days, accounting for the total number of samples of the corresponding regions at 16.58%, 21.70%, 27.18%, 17.89%, 6.63%, 25.67%. In the number of heavy pollution days above level III, Nanjing Metropolitan Circle and Hefei Metropolitan Circle have most of such days, followed by Suzhou-Wuxi-Changzhou Metropolitan Circle, Hangzhou Metropolitan Circle and Shanghai, with Ningbo Metropolitan Circle having the fewest such days.

The box plot of the temporal (monthly) variations of various pollutants in YRD is shown in Figure 3. As demonstrated, $PM_{2.5}$ was the major pollutant from November to March. However, in more than 30% of summer days (April-September) O_3 was the main pollutant due to more intensive photochemical reactions because of high temperature and solar radiation (Kalabokas et al. 2020). SO_2 and NO_2 had the lowest concentrations, which may be due to their role in the formation of secondary particulate matter and ozone (Manju et al. 2018).

Because $PM_{2.5}$ and ozone were the major pollutants during our study period, we investigated the temporal trend between AQI and them (Figure 4). The results show that contrary to ozone, which showed low correlation with

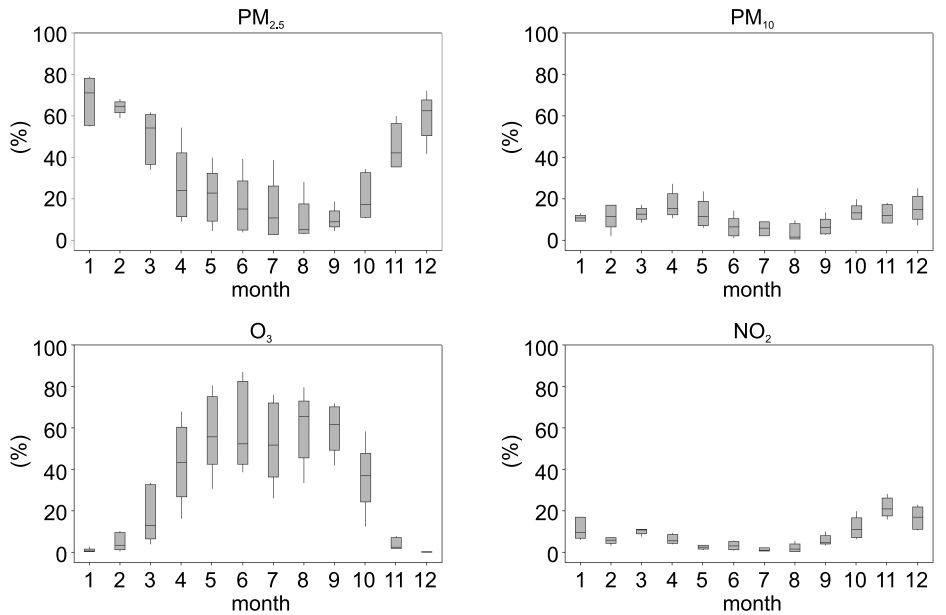

Fig. 3. Box plots of percentage of days with different air pollutants in the urban agglomeration in the YRD from 2014 to 2018. The line in the box represents the median, the upper and lower lines of the box represent the first percentile (Q1) and the third percentile (Q3), and the upper and lower whisker values represent the maximum and minimum values, respectively

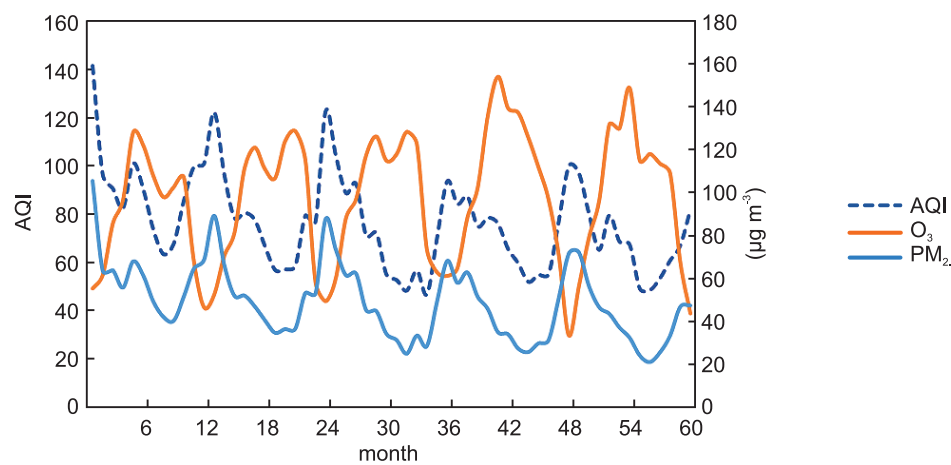

Fig. 4. Temporal correlation analysis between AQI and $PM_{2.5}$, O_3 in YRD from 2014 to 2018

AQI, the trend of AQI is consistent with that of $PM_{2.5}$. This indicates $PM_{2.5}$ is the major pollutant, which has strong influence on air quality of YRD region (Fu et al. 2018, Guo et al. 2019).

Time distribution features

Considering temperature variations, we defined four seasons as spring (10-22°C, April-May), summer (>22°C, June-September), autumn (22-10°C, October-November) and winter (<10°C, December-March). Monthly variation of AQI in the six regions of YRD is illustrated in Figure 5. It shows that the monthly variations of AQI develops a similar trend for the different regions, with the highest AQI in winter and the lowest one in summer. In winter, the atmospheric structure is stable and the temperature inversion under the boundary layer happens frequently. These conditions, accompanied by low precipitation, are favorable to the accumulation of pollutants near the earth's surface. Consequently, air pollutant concentrations are high in winter (Jassim et al. 2018). Conversely, in summer, the research area is affected by the southeast monsoon from the Pacific Ocean and the southwest monsoon from the Indian Ocean, which bring considerable rainfall. Therefore, the frequently rainy and windy weather is conducive to the diffusion of pollutants.

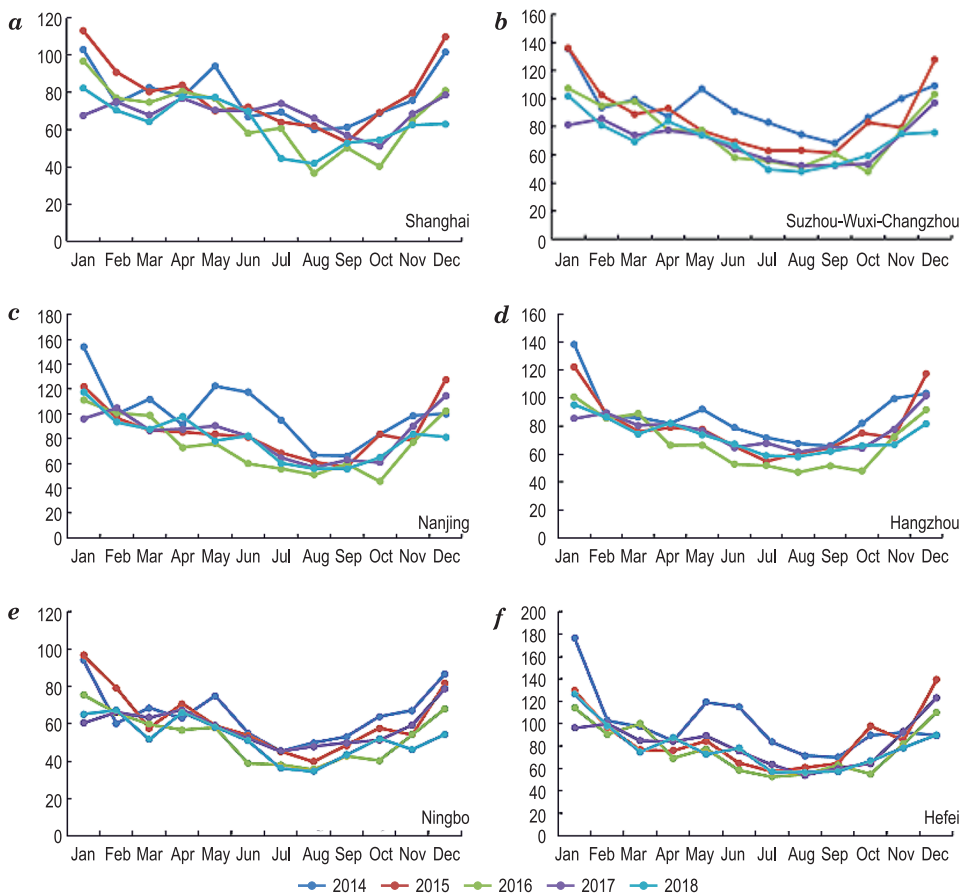

Fig. 5. Monthly variations of the air quality index (AQI) in YRD

At the same time, as the leaf area increases significantly, moist leaves in humid air are the best at the absorption and retention of particulate matter (Qi et al. 2019).

Spatial differentiation features

Due to the fact that the AQI value of some areas in Anhui has only been monitored since 2015, in order to ensure the consistency of the data, we produced the surface distribution of AQI based on the air monitoring data in 26 cities in YRD during a four-year period from 2015 to 2018. Data in Table 1 prove that the Ordinary Kriging (OK) method showed better performance with RMSE = 1 than inverse distance weight interpolation (IDW) or global polynomial interpolation (GPI).

Table 1

Comparison of interpolation results

Month	OK (MSE)	OK (RMSE)	IDW (MSE)	IDW (RMSE)	GPI (MSE)	GPI (RMSE)
January 2015	0.050	1.007	3.651	14.50	0.737	17.70
April 2015	0.031	1.094	1.383	8.782	0.247	11.07
July 2015	0.006	0.865	1.170	8.887	0.242	10.07
October 2015	-0.02	1.097	1.014	8.105	0.192	8.545
January 2016	0.103	1.457	1.136	9.165	0.027	8.086
April 2016	0.018	0.976	0.453	7.600	0.153	8.098
July 2016	0.043	1.576	1.794	10.82	0.482	14.38
October 2016	0.008	0.920	0.585	5.369	0.125	5.026
January 2017	0.041	0.843	-0.80	12.00	-0.10	9.404
April 2017	0.120	0.910	1.346	6.733	0.341	7.631
July 2017	0.061	1.132	2.650	16.33	0.604	17.17
October 2017	0.033	0.941	0.392	4.211	0.103	4.273
January 2018	-0.02	0.947	3.196	12.43	0.454	11.64
April 2018	0.065	0.942	2.142	10.28	0.428	11.59
July 2018	0.063	1.000	3.153	12.45	0.578	13.66
October 2018	-0.01	0.975	0.273	4.335	0.026	3.545

Note: OK –the Ordinary Kriging method, IDW – inverse distance weight interpolation, GPI – global polynomial interpolation, RMSE – Root Mean Square Error, MSE – Mean Absolute Error.

Figure 6 shows the seasonal surface distribution of AQI from 2015 to 2018 using OK method. Generally speaking, the AQI is higher in the northern regions of YRD than other regions. In YRD, Ningbo Metropolitan Circle had the lowest AQI (better air quality) followed by Shanghai, Hangzhou, Suzhou, Nanjing and Hefei respectively. In winter, AQI has an annually decreasing trend and the maximum value appeared in northern regions (Suzhou-Wuxi-Changzhou) in 2015 (AQI = 113). In spring, the worst air quality was observed in 2017. This can be explained by the severe storms (due to low humidity) happened in 2017 (Huo et al. 2019). Generally speaking, the YRD region is mostly affected by the natural dusts in the middle

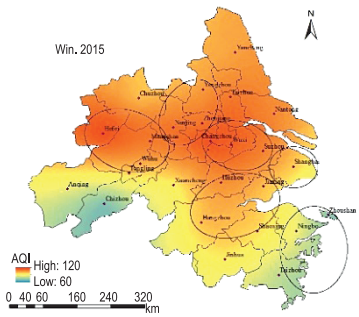
Win. 2015
N
AQI
High: 120
Low: 60
0 40 60 160 240 320
km

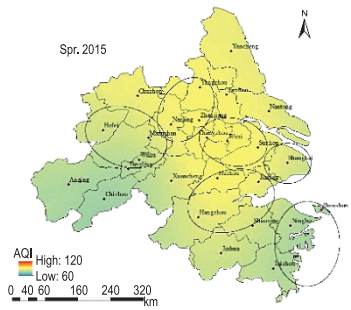
Spr. 2015
N
AQI
High: 120
Low: 60
0 40 60 160 240 320
km

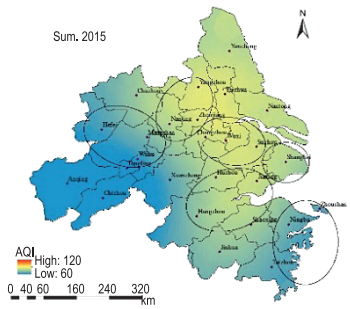
Sum. 2015
N
AQI
High: 120
Low: 60
0 40 60 160 240 320
km

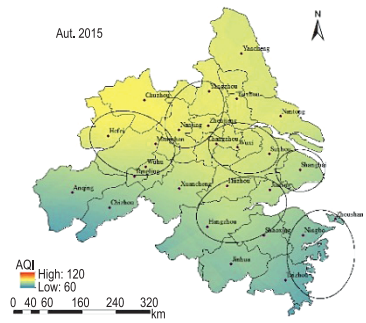
Aut. 2015
N
AQI
High: 120
Low: 60
0 40 60 160 240 320
km

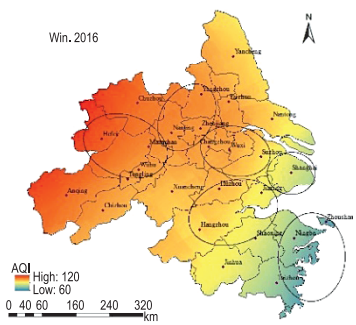
Win. 2016
N
AQI
High: 120
Low: 60
0 40 60 160 240 320
km

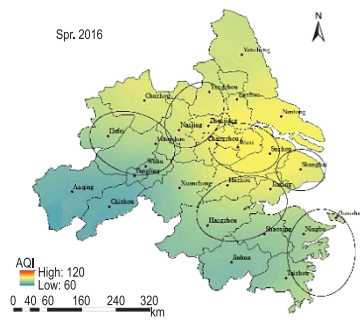
Spr. 2016
N
AQI
High: 120
Low: 60
0 40 60 160 240 320
km

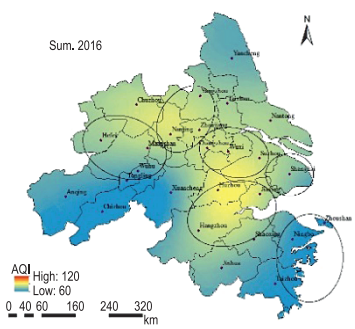
Sum. 2016
N
AQI
High: 120
Low: 60
0 40 60 160 240 320
km

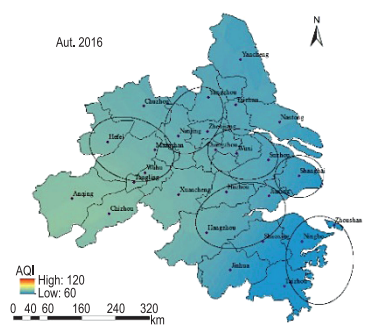
Aut. 2016
N
AQI
High: 120
Low: 60
0 40 60 160 240 320
km

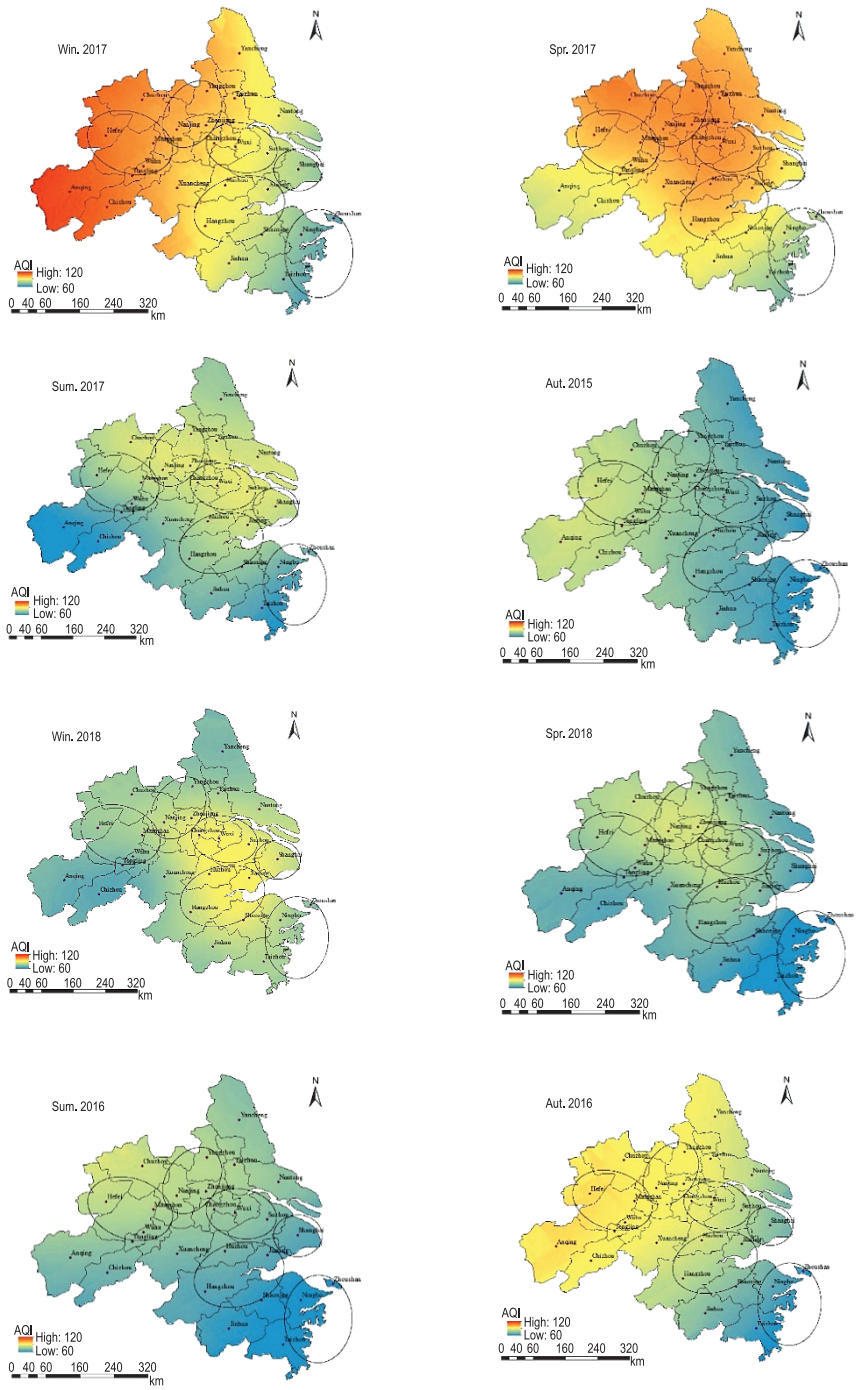

Fig. 6. Spatiotemporal distribution of AQI over YRD

and upper part of boundary layer that are transported from northern regions of YRD and cover the $PM_{2.5}$. Consequently, $PM_{2.5}$ concentrations increase and sever pollution can last for several days. In summer and autumn from 2015 to 2018, in inland cities (Suzhou-Wuxi-Changzhou, Hefei and Nanjing) AQI values showed an increasing trend. In spite of decreasing in the concentrations of pollutants such as particulate matter (because of the China air pollution controlling policy), the concentrations of O_3 has been rising and ozone is becoming the major pollutant in YRD during summer and autumn (HUANG et al. 2019). Therefore to improve the air quality of this region, more attempts should be done to reduce O_3 concentrations for the remediation of air pollution.

Relationship between air quality and meteorological elements

Correlation between AQI and meteorological parameters

We studied the trend of AQI and different meteorological parameters during our study period (Figure 7). As illustrated, the trends of air pressure

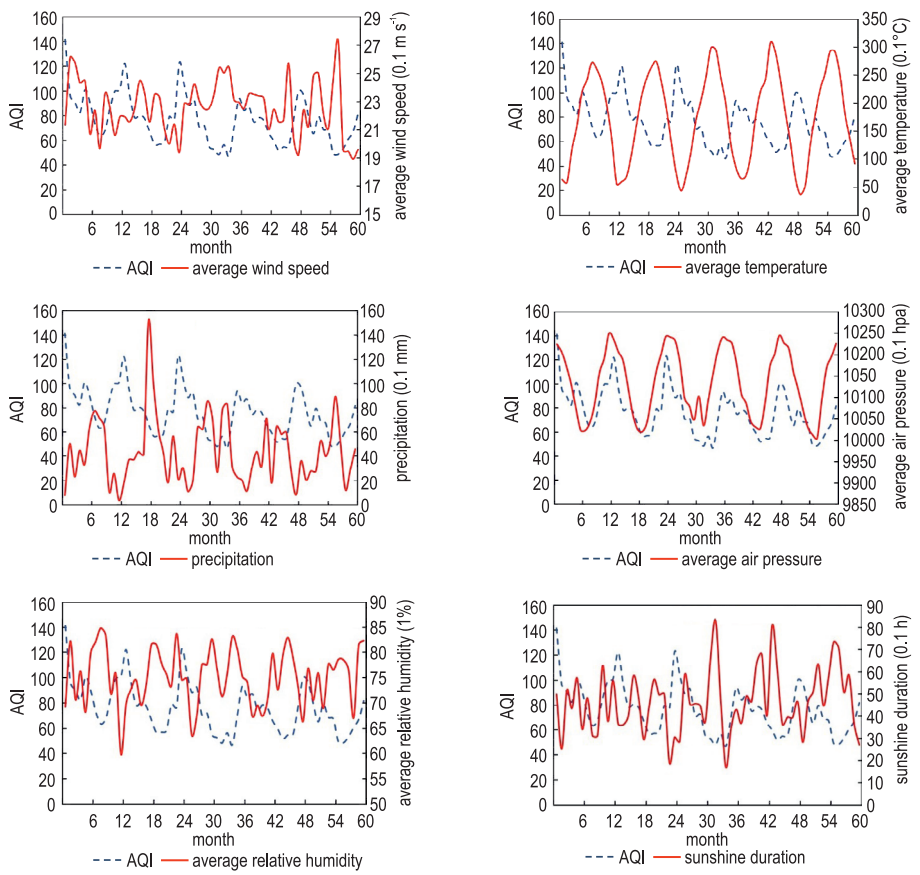

Fig. 7. Relationships between AQI and different meteorological parameters from 2014 to 2018

and AQI are remarkably consistent, indicating that pressure has a significant positive effect on the air quality in these cities. There is a significant negative correlation between the daily variation of AQI and the average temperature in 5 representative cities, from which it can be inferred that temperature has a positive effect on the air quality in the YRD region. This is because the diffusion of atmospheric pollutants in the vertical direction mainly depends on the vertical distribution of temperature. During our study period, Ningbo achieved the highest correlation coefficient (r=-0.428), followed by Hefei, Hangzhou, Nanjing and Shanghai.

Considering the effect of wind on air pollutant concentrations in YRD, we can classify winds into two categories: southeasterly and northwesterly ones. Northwesterly winds prevail in winter (dry season), with an average wind speed of 2.43 m s^{-1}, causing heavy dust pollution and consequently being negatively correlated with air quality. It can be inferred that humidity is one of the major parameters that influence air pollutants concentrations. Southeasterly winds mostly blow in summer and have lower average wind speed than northwesterly ones (almost 2 m s^{-1}) (Karimian et al. 2019). However, they have a positive impact on air quality by dispersing and removing pollutants. The correlation between precipitation and AQI is negative (the correlation coefficient is in the range of -0.284-0.210), which implicates that the air pollution in YRD contains water-soluble pollutants that can be washed away by rain. Moreover, the negative correlation between AQI and RH (-0.161 to -0.326) indicates that relative humidity is unfavorable for the formation of air pollution. There is no clear correlation between the duration of sunshine and AQI. This may be explained by the fact that, although sunshine accelerates the dilution of pollutants by increasing the boundary layer height, it affects the formation of secondary particulate matter by photochemical reactions (Karimian et al. 2017). It is worth mentioning that as each of these parameters is not the sole parameter governing concentrations of pollutants, the correlation coefficients are not high.

Prediction of AQI value in YRD

Figure 8 shows scatter plots of observed and predicted AQI using ARIMA (0,1,2) and MLR respectively. It proves that the ARIMA model showed better performance with overall RMSE=27.991 and R^2=0.45 than MLR (RMSE=33.414 and R^2=0.2707). There is reasonable agreement between ground truth and predicted values, and our ARIMA model is able to explain over 50% (R^2=0.51) of the variability in observed AQI. However, for different metropolitan areas, the slopes of linear regression are less than 1 and intercepts are positive. This illustrates a tendency of the model to underestimate and overestimate high and low AQI values, respectively.

Figure 9 illustrates the averaged surface distribution of ARIMA predicted and observed AQI from 11 July 2016 to 20 July 2016. Note that this period was selected randomly and was excluded from training datasets. Generally,

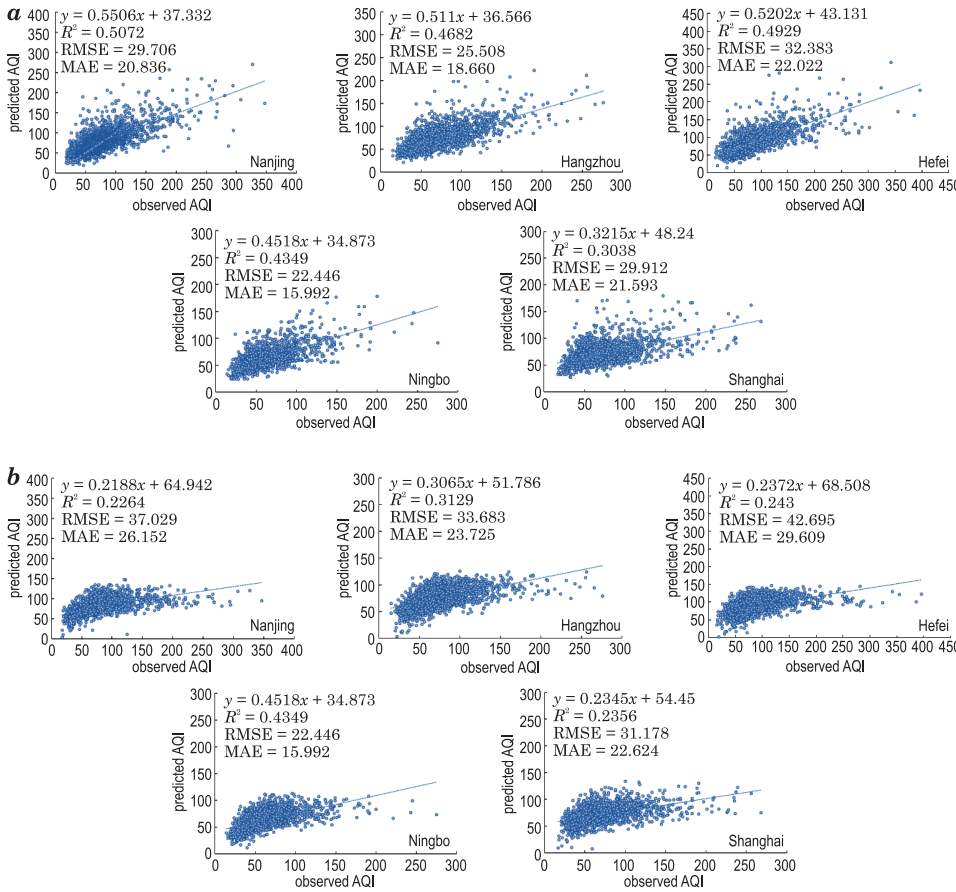

Fig. 8. Scatter plots of observed and predicted AQI by the ARIMA – *a*, the MLR – *b*

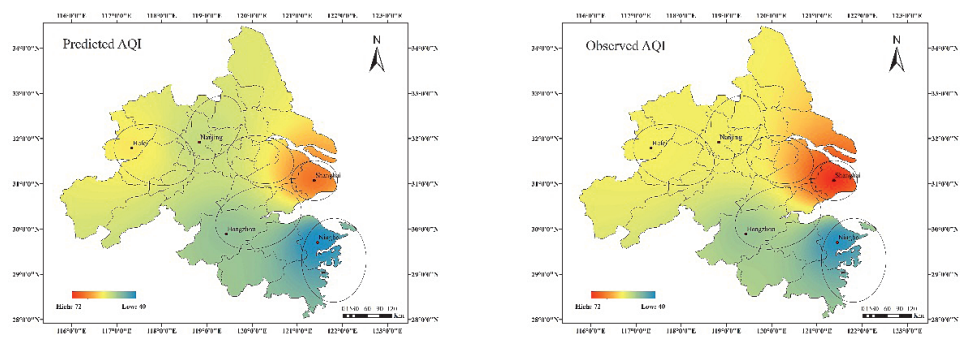

Fig. 9. Predicted AQI using ARIMA (0,1,2) and surface observed AQI

the predicted distribution pattern follows the observed one. However, same as the trend of the test dataset, our predicted surface shows a tendency towards underestimation.

CONCLUSIONS

In this paper, we studied AQI in the new YRD region composed of one core and five metropolitan areas. This is one of the earliest studies that have investigated air quality in YRD on such a large scale (spatially and temporally). Comparing different spatial interpolation methods, we found that Kriging outperforms other models (IDW, polynomial) in producing surface distribution of AQI. The results showed that the spatial distribution of AQI varied seasonally and except for winter, the AQI level did not exceed level II in almost the entire YRD area. Moreover, AQI showed a declining trend as an indicator of the air pollution controlling programs in China. Among all metropolitan cities in YRD, Ningbo had the best air quality while Hefei was the worst. Generally, the southern part of YRD had better air quality than the northern part, which could be explained by larger population density in the northern part as well as the distance from the sea. We also found that the winds blowing to YRD have opposite effects on air quality. Southeasterly winds (0.5-8.3 m s^{-1}) can improve the air quality, while northwesterly winds in dry season have negative impacts, causing heavy dust pollution in YRD. Our comparison of the models showed that the ARIMA (0,1,2) model has higher prediction accuracy than MLR, which is more suitable for AQI prediction over YRD. Future air pollution studies in this area should consider models which take into account spatial non-stationarity. Future work will deal with explanatory variables and include satellite-based data to detect air pollution emission sources in YRD for forecasting air pollutant concentrations.

REFERENCES

Adaes J., Pires J.C.M. 2019. *Analysis and modelling of PM2.5 temporal and spatial behaviors in European cities*. Sustainability-Basel, 11(21): 6019. DOI: https://doi.org/10.3390/su11216019

Adame J.A., Notario A., Cuevas C.A., Lozano A., Yela M., Saiz-Lopez A. 2019. *Recent increase in NO_2 levels in the southeast of the Iberian Peninsula*. Sci. Total Environ., 693. DOI: https://doi.org/10.1016/j.scitotenv.2019.133587

Baltaci H., Akkoyunlu B.O., Arslan H., Yetemen O., Ozdemir E.T. 2019. *The influence of meteorological conditions and atmospheric circulation types on PM10 levels in western Turkey*. Environ Monit Assess, 191: 466. DOI: https://doi.org/10.1007/s10661-019-7609-7

Borge R., Requia W.J., Yague C., Jhun I., Koutrakis P. 2019. *Impact of weather changes on air quality and related mortality in Spain over a 25 year period 1993-2017*. Environ. Int., 133: 14. DOI: https://doi.org/ 10.1016/j.envint.2019.105272

Chwil, S., Tkaczyk P., Chwil S., Kozłowska-Strawska J., Chwil P., Matraszek R. 2015. *Assessment of air pollutants in an urban agglomeration in Poland made by the biomonitoring of trees*. J. Elem., 20(4): 813-826. DOI: https: 10.5601/jelem.2015.20.1.742

Fenech S., Doherty R.M., Heaviside C., Macintyre H.L., O'Connor F.M., Vardoulakis S., Neal L., Agnew P. 2019. *Meteorological drivers and mortality associated with O_3 and $PM_{2.5}$ air pollution episodes in the UK in 2006*. Atmos. Environ., 213: 699-710. DOI: https://doi.org/ /10.1016/j.atmosenv.2019.06.030

Fu W.C., Chen Z.R., Zhu Z.P., Liu Q.Y., van den Bosch C.C.K., Qi J.D., Wang M., Dang E., Dong J.W. 2018. *Spatial and temporal variations of six criteria air Pollutants in Fujian Province, China*. Int. J. Environ. Res. Public Healt, 15(12): 20. DOI: https://doi.org/10.3390/ /ijerph15122846

Guo H., Sahu S.K., Kota S.H., Zhang H.L. 2019. *Characterization and health risks of criteria air pollutants in Delhi, 2017*. Chemosphere, 225: 27-34. DOI: https://doi.org/10.1016/j.chemosphere.2019.02.154

Hrishikesh C.G., Nagendra S.M.S. 2019. *Study of meteorological impact on air quality in a humid tropical urban area*. J. Earth Syst. Sci., 128(5):118. DOI: https://doi.org/10.1007/s12040--019-1116-7.

Huang X., Shao T., Zhao J., Cao J., Song Y. 2019. *Spatio-temporal differentiation of ozone concentration and its driving factors in Yangtze River Delta Urban Agglomeration*. Resources and Environment in the Yangtze Basin, 28(06): 1434-1445. (in Chinese) DOI: 10.11870/ /cjlyzyyhj201906018

Huo Y., Deng X., Gong Z., Yang G., Sun Q., Zhai J., Yu C. 2019. *Formation analysis of a heavy dust pollution event in the Yangtze River Delta in May 2017*. J. Meteor. Environ., 35(1): 26-34. (in Chinese) DOI: 10.3969/j.issn.1673503X.2019.01.004

Jassim M.S., Coskuner G., Munir S. 2018. *Temporal analysis of air pollution and its relationship with meteorological parameters in Bahrain, 2006-2012*. Arab. J. Geosci., 11(3): 15. DOI: https://doi.org/ 10.1007/s12517-018-3403-z

Kalabokas P., Jensen N.R., Roveri M., Hjorth J., Eremenko M., Cuesta J., Dufour G., Foret G., Beekmann M. 2020. *A study of the influence of tropospheric subsidence on spring and summer surface ozone concentrations at the JRC Ispra station in northern Italy*. Atmos. Chem. Phys., 20(4): 1861-1885. DOI: https://doi.org/ 10.5194/acp-20-1861-2020

Karimian H., Li Q., Li C., Chen G., Mo Y., Wu C., Fan J. 2019. *Spatio-temporal variation of wind influence on distribution of fine particulate matter and its precursor gases*. Atmos. Pollut. Res., 10(1): 53-64. DOI: https://doi.org/10.1016/j.apr.2018.06.005

Karimian H., Li Q., Li C.C., Fan J., Jin L., Gong C., Mo Y., Hou J., Ahmad A, 2017. *Daily estimation of fine particulate matter mass concentration through satellite based aerosol optical depth*. ISPRS J. Photogramm., IV-4/W2: 175-181. DOI: 10.5194/isprs-annals-IV-4-W2-175-2017

Li K.,. Chen L, Fang Y., White S.J., Jang C., Wu X., Gao X., Hong S., Shen J., Azzi M. 2017. *Meteorological and chemical impacts on ozone formation: A case study in Hangzhou, China*. Atmos. Res., 196: 40-52. DOI: https://doi.org/10.1016/j.atmosres.2017.06.003

Li X., Wang D., Lu Q., Peng Z., Fu Q., Hu X., Huo J., Xiu G., Li B., Li C., Wang D., Wang H. 2018. *Three-dimensional analysis of ozone and $PM_{2.5}$ distributions obtained by observations of tethered balloon and unmanned aerial vehicle in Shanghai, China*. Stoch. Env. Res. Risk A., 32(5): 1189-1203. DOI: https://doi.org/10.1007/s00477-018-1524-2

Manju A., Kalaiselvi K., Dhananjayan V., Palanivel M., Banupriya G.S., Vidhya M.H., Panjakumar K., Ravichandran B. 2018. *Spatio-seasonal variation in ambient air pollutants and influence of meteorological factors in Coimbatore, Southern India*. Air Qual. Atmos. Hlth., 11(10): 1179-1189. DOI: https://doi.org/10.1007/s11869-018-0617-x

Mo Y., Li Q., Karimian H., Fang S., Tang B., Chen G., Sachdeva S. 2020. *A novel framework for daily forecasting of ozone mass concentrations based on cycle reservoir with regular jumps neural networks*. Atmos. Environ., 220. DOI: https://doi.org/10.1016/j.atmosenv. 2019.117072

Nowak D.J., Hirabayashi S., Doyle M., McGovern M., Pasher J. 2018. *Air pollution removal by urban forests in Canada and its effect on air quality and human health*. Urban For. Urban Green, 29**:** 40-48. DOI: https://doi.org/10.1016/j.ufug.2017.10.019

Qi Y., Li Q., Karimian H., Liu D. 2019. *A hybrid model for spatiotemporal forecasting of PM2.5 based on graph convolutional neural network and long short-term memory*. Sci. Total. Environ., 664**:** 1-10. DOI: https://doi.org/10.1016/j.scitotenv.2019.01.333

Wang J., Zhang X., Li D., Yang Y., Zhong J., Wang Y., Che H., Che H., Zhang Y. 2018. *Interdecadal changes of summer aerosol pollution in the Yangtze River Basin of China, the relative influence of meteorological conditions and the relation to climate change*. Sci. Total Environ., 630**:** 46-52. DOI: https://doi.org/10.1016/j.scitotenv.2018.01.236

Zhang H., Cheng X., Chen R. 2018. *Analysis on the spatial-temporal distribution characteristics and key influencing factors of $PM_{2.5}$ in Anhui Province*. Acta Sci. Circumst., 38(3): 1080-1089. (in Chinese) DOI: 10.13671/j.hjkxxb.2017.0486

Zheng C., Zhao C., Li Y., Wu X., Zhang K., Jing G., Qi Q., Ren Y., Xi Z., Chai F. 2018. *Spatial and temporal distribution of NO_2 and SO_2 in Inner Mongolia urban agglomeration obtained from satellite remote sensing and ground observations*. Atmos. Environ., 188: 50-59. DOI: https://doi.org/10.1016/j.atmosenv.2018.06.029